Thermal Design and Performance results of the first High-Beta Cryo-module for HIE-ISOLDE at CERN

2015 IOP Conf. Ser.: Mater. Sci. Eng. 101 012045

(http://iopscience.iop.org/1757-899X/101/1/012045)

Thermal Design and Performance results of the first High-Beta Cryo-module for HIE-ISOLDE at CERN

L Valdarno, N Delruelle, Y Leclercq, V Parma, G Vandoni, L Williams

CERN, Geneva 23, CH-1211 Switzerland

E-mail: luca.valdarno@cern.ch

Abstract. The High Energy and Intensity HIE-ISOLDE is a facility under construction at CERN whose target is ultimately, after the installation of six cryo-modules, to produce radioactive ion beams at 10MeV/u maximum energy in order to significantly expand the nuclear physics programme carried out by REX-ISOLDE. Since thermal control is essential to the performance of the whole cryo-module, a combination of a passive (materials, coatings, and surface finishes) and active (cryogenic loops, heaters) control has been designed to keep the cryostat operating within the allowable thermal budget. A numerical model based on Finite Element has been developed in order to generate a faithful global mapping of temperatures and heat fluxes inside the cryo-module. The numerical model, combined with the experimental results of the first test campaign, will serve as an optimization tool for the future cryo-modules in terms of improvement in the global and specific heat loads management.

1. Introduction

The HIE-ISOLDE facility will be equipped with two low-β and four high-β cryo-modules each containing superconducting niobium sputtered Quarter Wave Resonators and superconducting solenoid magnets. The assembly of the first high-β cryo-module has started in late August 2014 in a dedicated class100 (ISO5) clean room equipped with specific tooling [1]. It was delivered to the HIE-ISOLDE beam line in early May 2015 to provide an optimised vacuum and cryogenics environment and to offer the highest beam quality output to the scientific community for a first physics run due to start by the end of 2015 [2]. This first unit has been connected to the cryogenic distribution line and its performance is being tested and validated during summer 2015.

In this paper the layout of the thermal control system and the global thermal analysis of the cryo-module together with some advanced studies on particular components will be presented and discussed. The implemented Finite Element (FE) model has as primary aim to reproduce as precisely as possible the most significant heat exchange phenomena, but it also represents a validation and diagnostic tool for interpreting the experimental data obtained from numerous temperature sensors located inside the cryostat and once benchmarked, may be used to simulate and explain cryo-module performance outside nominal conditions.

2. HIE-ISOLDE high-beta cryo-module

The HIE-ISOLDE high-β cryo-module, shown in Figure 1, houses five superconducting ¼ wave cavities and one superconducting solenoid magnet all operating in liquid helium at 4.5 K. The components and subsystems comprising the cryo-module, their specific characteristics and expected performance are detailed in [3]. In order to provide the best operational environment for the radioactive ion beams, the cryo-module is designed to maintain stable operating conditions for the five superconducting cavities and the solenoid magnet. For this reason, throughout its operational life, the cryo-module has to fulfil the following core requirements:

- Accurate alignment and precise location within 0.3mm for the RF cavities and 0.2mm for the solenoid magnet with respect to the beam axis;
- Cleanliness of the surfaces of the RF cavities in order to preserve their performance, extremely sensitive to particulate contamination;
- Thermally insulate from heat in-leaks within budgets;
- Ultra High Vacuum ($<10^{-8}$ mbar at cold) and leak tightness to better than $1\text{x}10^{-11}$ Pa m^3 s^{-1}.

All these requirements have not only been fundamental in the design and manufacture of the cryo-module components, but also in the definition of the operational phases starting from the first cool-down to steady-state conditions and during warm-up. In particular, since no Multi-Layer Insulation (MLI) could be used, a bare copper thermal shield electroplated with a 15μm of nickel has been chosen in order to have an easily cleanable (ISO5 compatible), oxide free and low emissivity that could preserve also the cleanliness of the cavities surfaces.

In order to monitor and control the alignment of the cavities and solenoid during operation, the Mathilde system [4] optically monitors the absolute positions on the reference beam axis and if necessary allows position correction via external adjusters to be made with respect to the beam line. Mathilde is based on CCD cameras, mounted outside the cryo-module, flashing through viewports and receiving reflected beams of light from the targets mounted on supporting referential structures, so called "Omega plates", placed under the support frame (see Figure 1).

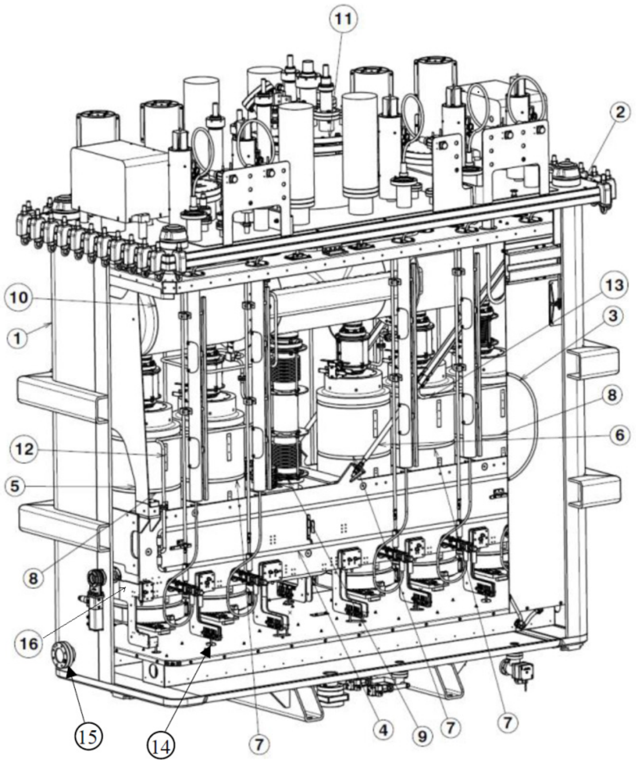

Figure 1. The complete HIE-ISOLDE high-β cryo-module: 1 Vacuum vessel lower box, 2 Vacuum vessel top plate assembly, 3 Thermal shield lower box, 4 Support frame, 5 Suspension end plate, 6 Tie-rod, 7 Inboard cavity, 8 Outboard cavity, 9 Down tube to solenoid, 10 Helium vessel, 11 Chimney assembly, 12 Support frame cooling supply, 13 Support frame cooling return, 14 Mathilde targets, 15 Mathilde viewport, 16 Omega plate.

3. Global heat transfer performance

The purpose of a thermal management system is to maintain all cryo-module components within the allowable temperature limits for all operating modes and consequently to guarantee the performance of the overall system. Moreover it is necessary to ensure during transients, that the temperature gradients remain under defined limits, in order to avoid local plastic deformation of the materials, induced distortions and permanent misalignment of the cavities and solenoid. The trade-offs on the general design, also based on the optimization of the heat leaks throughout the cryo-module, are presented and discussed in [3].

In steady-state mode, two independent cryogenic circuits, a 50-75 K gaseous helium line and a 4.5 K GHe-LHe transfer line, provide a continuous active thermal control. The five RF superconducting cavities, dissipating a nominal heat of 10W each, and the solenoid are connected to the helium reservoir and filled with liquid helium at 4.5 K constant temperature and 1.3 bars pressure. The helium reservoir is kept half filled with liquid helium and vapour pumping at constant pressure ensures that a constant temperature of 4.5 K is maintained. An estimated helium mass flow between 3 and 4 g/s, injected into the cooling circuit on the thermal shield, extracts a total corresponding power between 310-360 W. With an assumption of an emissivity of 0.033 on the shield and 0.2 on the vacuum vessel, the estimated radiative heat exchange is 190 W. Figure 2 presents a schematic of the main components of the cryo-module with static and dynamic heat transfer.

The cryo-module is also equipped with several heaters (50 W each) on the cavities and in the reservoir for temperature control reasons, namely to accelerate warm-up transients. In order to continuously monitor the status of the cryo-module throughout the transient phases and in the steady-state status, fifty Cernox temperature sensors are located at strategic points on the structure.

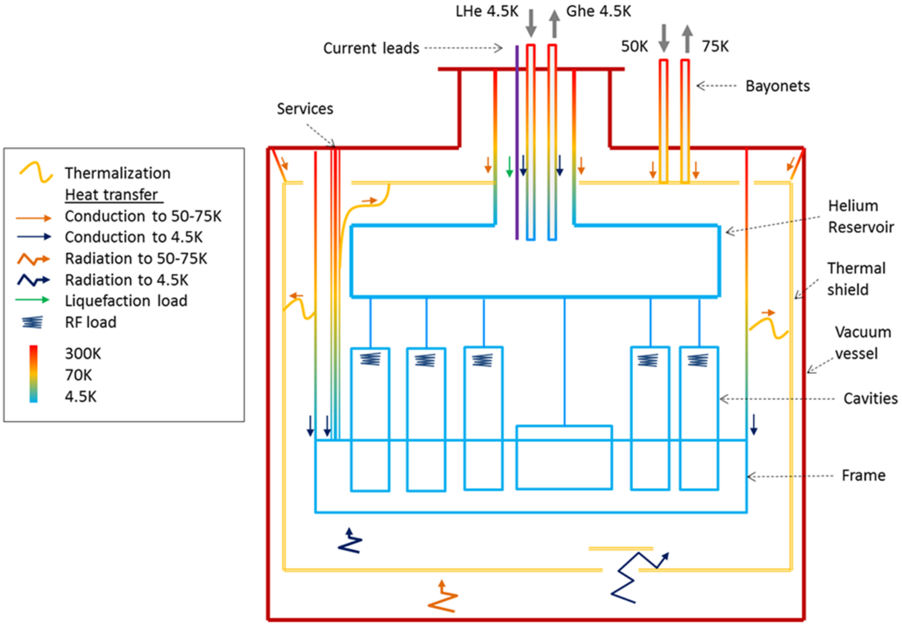

Figure 2. Schematic of heat transfer inside the cryo-module.

Components and incoming services are thermalized on the top of the thermal shield to reduce the heat transfer through conduction to the 4.5 K level but also to reduce thermal transients on structural elements. Several copper strip thermalisations have been designed and placed in strategic places in the cryo-module to enhance temperature uniformity. The stainless steel tie-rods supporting the frame have been equipped with copper strips cooled via the thermal shield in order to accelerate cooling of these structures and reduce the cool-down transient. The same design philosophy has been applied to the RF cables, thermalized along the shielding tube, and to the omega plates, mechanically connected to the support frame. The overall conductive heat load is estimated at around 120 W at 50-75 K, all inclusive (thermal shield supports, all the thermalisations, RF pick-up, and instrumentation). The solenoid is powered via a pair of resistive current leads operating at a maximum current of 120A, and helium vapour cooled at a corresponding rate of 0.02 g/s. Table 1 shows the estimation of static and dynamic heat loads acting on the cryo-module in steady-state mode. This estimation is based on assumptions on the emissivity of the thermal shield, efficiency of lower tunnels anodised walls, radiative taps and influence of assembly issues that have to be tested yet. The radiation exchange between the vacuum vessel and the thermal shield, and the dynamic heat load are respectively the highest contributions in the GHe and GHe-LHe circuits.

Table 1. Estimation of static and dynamic heat loads in steady-state mode.

	GHe circuit @ 50K-75K [W]	GHe-LHe circuit @ 4.5K [W]	Current leads @ 4.5K-300K [g/s]
Radiation	190	2	-
Conduction	120	16	-
Dynamic load	52	52	0.02
Total static mode	310	18	-
Total dynamic mode	362	70	0.02

4. Thermal model

The performance of the entire cryo-module and of its single parts has been accurately modelled and analysed through a Finite Element model built on ANSYS in agreement with the European Cooperation for Space Standardization (ECSS) recommendations [5]. A preliminary correlation between analysis and test results has been performed in order to substantiate the adequacy of the FE model to simulate the thermo-mechanical behaviour measured during the test on the actual hardware. The complete validation of the FE model will be carried out as soon as all the experimental data coming from the different thermal modes is available.

During the cool-down the thermal shield receives radiative heat flux from both the external vacuum vessel and from the internal cold mass. The top plate, on which the gaseous helium inlet and outlet are located, presents the temperature gradient most critical to the structural response of the shield. The thermo-mechanical behaviour of the thermal shield top plate during cool-down transients is shown in Figure 3. During this phase the maximum thermal excursion across the thermal shield top plate is controlled to remain below 50 K, in order to ensure a maximum von-Mises stress of 30 MPa.

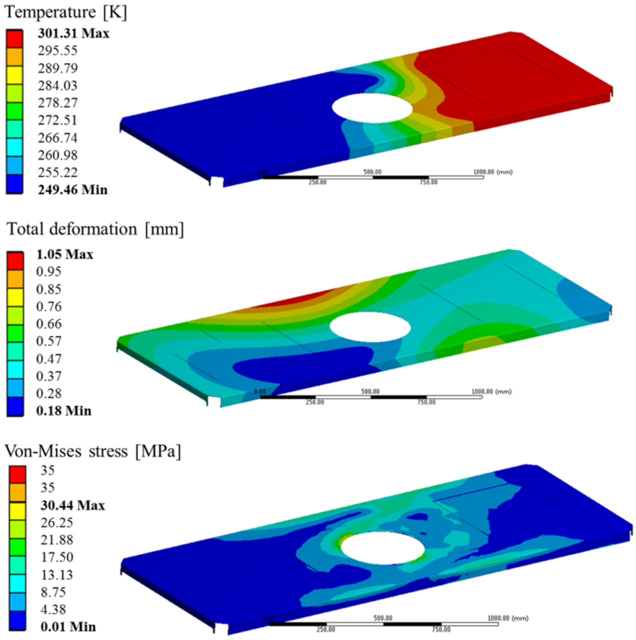

Figure 3. Thermo-mechanical behaviour of the upper panel of the thermal shield (ANSYS).

During cool-down of the frame, a heat extraction of 100 W per side (Q= $\dot{m}c_p\Delta T$) has been considered a reasonable compromise in order to keep stresses and deformation within safe limits. The temperature sensors, located along the cryogenic cooling line, and data from the Mathilde system allow this phase to be monitored and controlled to avoid excessive deformations and stresses in the structure. As an example, if the temperature sensors on some particular positions on the frame show a ΔT_{max} higher than 40 K, the cooling mass flow inside the circuit is stopped allowing temperatures to diffuse and become uniform throughout the frame. Furthermore, in order to avoid excessive differential thermal contraction between the helium reservoir and the frame, which may induce excessive displacements of the cavities and solenoid bellows, the maximum temperature difference between the two components is kept below 100 K.

Figure 4 shows the temperature changes of the main components of the cryo-module during its first cool-down, which has been carried out slowly and uniformly starting on June 4th till June 18th. During its first phase the thermal shield circuit is gradually cooled by helium gas from 250 K in an initial stage, down towards 50 K, while in the meantime the inner components are homogenously cooled by simple radiation. Afterwards, in the second phase, the helium gas leaving the thermal shield has been injected also into the support frame circuits and then into the helium reservoir, increasing the overall cooling rate. It is possible to observe how the temperatures on the frame and reservoir drop quite rapidly and cool down together avoiding differential temperature distortions. An incidental warm-up has taken place during the early morning of 11th of June, when a spurious reading of a temperature interlock caused the cooling to stop and the temperature increase of the thermal shield of 50K in four hours. In the final phase, the frame, the reservoir, followed finally by the cavities and the solenoid are cooled to 4.5 K in order to reach their steady state condition through a direct injection of liquid helium.

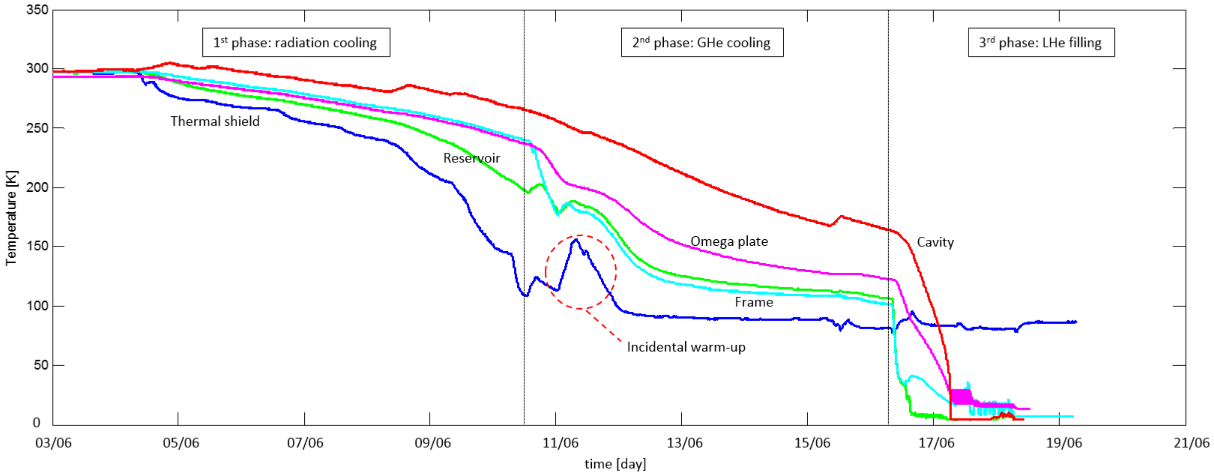

Figure 4. First cool-down of the cryo-module.

Figure 5 (left) shows a good correlation between the experimental data and the numerical simulation of the radiation cooling phase performed with the FE model. In particular it is interesting to note the effect of the RF powering (at the beginning of day 3) of the cavities to keep them warmer than the rest of the structure resulting in a temperature rise of about 10 K.

In order to facilitate the temperature distribution by simple conduction along the structure, two thermalisations are mechanically connected between the support frame and each omega plate. It is possible to observe in Figure 5 (right) how this thermalisation has improved the temperature management forcing the omega plates to follow more closely the behaviour of the frame rather than being cooled by radiation alone.

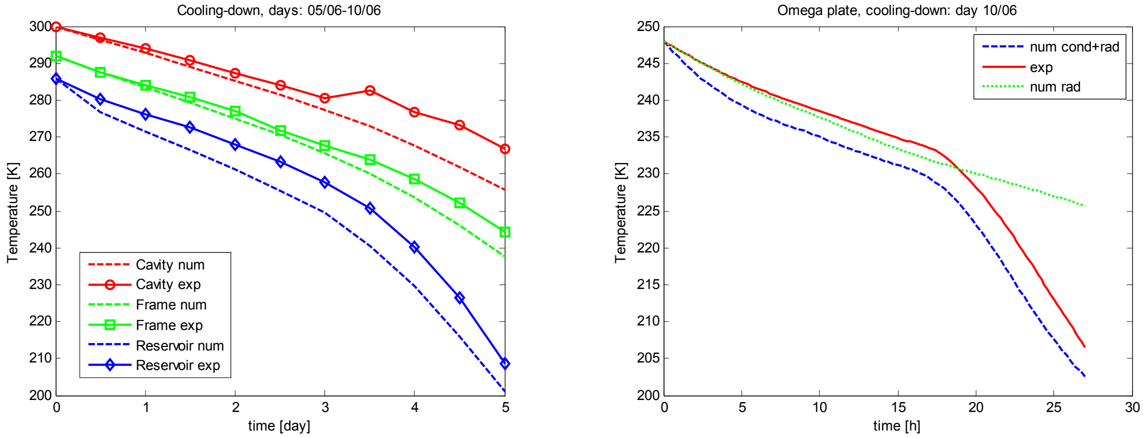

Figure 5. Experimental and numerical temperature behaviours: global (left), omega plate (right).

During the cool-down the Mathilde system has continuously measured the displacements of the reference points on the targets attached to the omega plates. At the end of the transient phase the overall maximum contraction is 5.5mm vertically, with 1mm of displacement at the target level with respect to the beam line, all in agreement with the thermo-mechanical calculations.

5. Current leads and solenoid splices

The cryogenic heat load due to solid conduction and ohmic heating in the resistive leads has to be optimised in order to minimise helium boil-off and the liquefaction inventory.
Commercially available resistive gas cooled current leads of 200A capacity have been used and modified to extend their length as shown in Figure 6. A first OFE copper strip extension, about 25 cm long, carry the current down to the liquid level in the helium vessel and a further extension of about 100 cm, up to the solenoid is made using a Nb-Ti superconducting wire that is constantly immersed in the helium bath. The electrical splice connection to the solenoid wires is made by mechanical clamping with a bolted connection assembled with a given torque to minimize the electrical resistance.

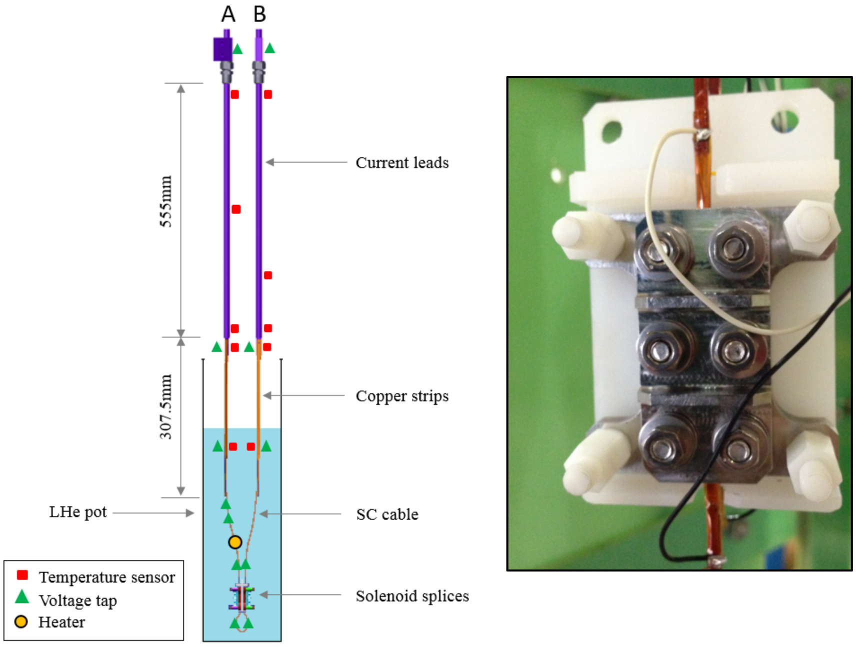

Figure 6. Layout of the experimental setup for the current leads (left), solenoid splice (right).

The performance of the two resistive vapour-cooled current leads powered within a 10-200A current range and vapour cooled by a 0.01-0.09 g/s mass flow has been tested in a dedicated set-up in a vertical test cryostat. The aim of these performance tests is not only to evaluate the behaviour of the current leads under operational conditions, but also to measure the contact resistance of the mechanical splice connecting the superconducting wire in 4.5 K liquid helium and assess its stability after thermal cycles. Each current lead is instrumented with temperature sensors and several voltage taps along the line which give information on the evolution of the splice electrical resistance as a function of the current, gas flow and level of the liquid helium (see Figure 6).

Assuming a steady state condition and neglecting thermal conduction in the gas, the system of the current lead can be modelled in the one-dimensional case as:

$$\frac{d}{dx}\left(k(T)A\frac{dT}{dx}\right) = -\frac{\rho(T)I^2}{A} + Ph(T)(T-\vartheta) \tag{1}$$

$$\dot{m}c_p(\vartheta)\frac{d\vartheta}{dx} = Ph(T)(T-\vartheta) \tag{2}$$

where k and ρ are respectively the thermal conductivity and the electrical resistivity, A and P are the cross-section and the wetted perimeter of the current lead, ϑ temperature of the gas, c_p specific heat of the gas, $\dot{m}$ gas mas flow rate and h heat exchange coefficient.

As shown in Figure 7 (left), numerical calculations are confirmed by a high measured temperature gradient just in the top quarter of the lead with an almost uniform temperature equal to the temperature of the liquid bath over the remaining length. Figure 7 (right) illustrates how the temperature at the top of the current lead is dependent on the mass flow rate and on the ohmic heating due to the supply current.

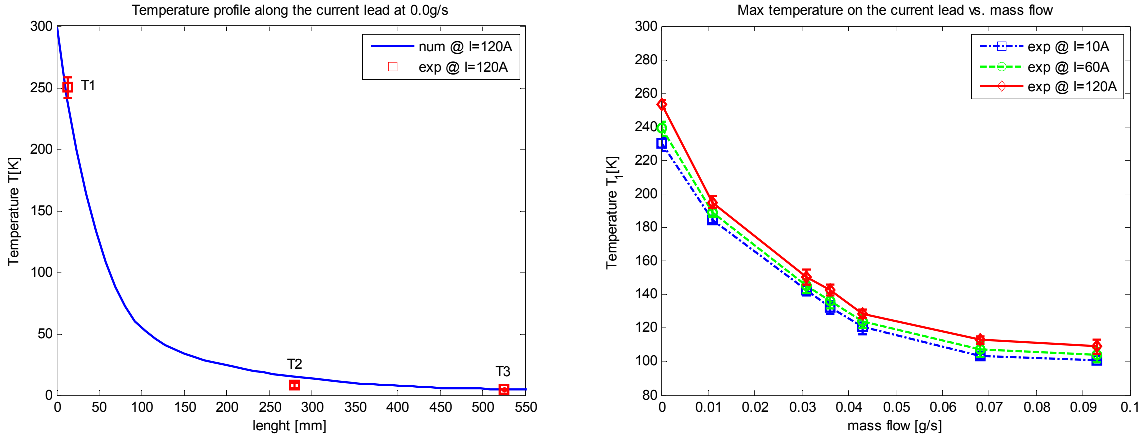

Figure 7. Temperature profile along the current lead (left), Temperature behaviour at the top of the current lead at different mass flows (right).

The helium mass flow inside the current lead has the effect of decreasing the electrical resistance from 0.65 mΩ, when it is not actively cooled, to 0.25 mΩ with a 0.02 g/s mass flow, improving the thermal efficiency of the lead. The electrical resistance of the solenoid splice is 20±3 nΩ, variable according to the torque applied to the nuts on the six threaded studs that apply compressive force through spring washer to the mechanical joints. A quench on the SC cable has been induced by powering a cable attached spot heater in range between 0.5-2.5 W. A rapid decrease of the post-quench level of the liquid helium bath has been observed, followed by a loss of the superconducting properties of the cable.

6. Conclusions

The first high-β cryo-module has been successfully delivered and installed on the HIE-ISOLDE beam-line for complete functional tests taking place during summer 2015. The first cool-down of the system to steady state operational conditions has been completed by mid-June 2015.

A preliminary analysis of the first cool-down data demonstrates the validity of the numerical analysis performed on ANSYS. Once a complete set of experimental data has been gathered, it will serve to completely benchmark the FE model. This simulation tool provides information not only on the nature of the heat exchange phenomena and their effect on the structural stability of the internal components of the cryo-module, but also represents an optimization tool for future cryo-modules to improve the global and local heat load management.

Acknowledgements

The authors would like to acknowledge for the support from the HIE-ISOLDE project management and all colleagues who have kindly contributed to the material presented in this paper.

References

[1] Y. Leclercq et al., "The Assembly experience of the first Cryo-module for the HIE-ISOLDE at CERN" in *IPAC*, Richmond, USA, 2015.

[2] Y. Kadi et al., "HIE-ISOLDE: the future of Radioactive Beam Physics at CERN", editors S. Myers et al., 2015 (in publication) .

[3] L. Williams et al., "The high Beta cryo-modules and the associated cryogenic system for the HIE-ISOLDE" in *CEC/ICMC13*, Anchorage, June 2013.

[4] G. Kautzmann et al., "HIE-ISOLDE - General presentation of Mathilde" in *IWAA 2014*, Beijing, October 2014.

[5] European Cooperation for Space Standardization, “Structural finite element models” ESA/ESTEC, Noordwijk, The Netherlands, July 2008.